A Modeling Approach for Investigating Opto-Mechanical Relationships in the Human Eye Lens

Kehao Wang, Demetrios T. Venetsanos, Masato Hoshino, Kentaro Uesugi, Naoto Yagi, and Barbara K. Pierscionek

Abstract*—*Objective: **The human visual system alters its focus by a shape change of the eye lens. The extent to which the lens can adjust ocular refractive power is dependent to a significant extent on its material properties. Yet, this fundamental link between the optics and mechanics of the lens has been relatively under-investigated. This study aims to investigate this opto-mechanical link within the eye lens to gain insight into the processes of shape alteration and their respective decline with age.** ***Methods:*** **Finite Element models based on biological lenses were developed for five ages: 16, 35, 40, 57, and 62 years by correlating *in vivo* measurements of the longitudinal modulus using Brillouin scattering with *in vitro* X-ray interferometric measurements of refractive index and taking into account various directions of zonular force.** ***Results:*** **A model with radial cortical Young's moduli provides the same amount of refractive power with less change in thickness than a model with uniform cortical Young's modulus with a uniform stress distribution and no discontinuities along the cortico-nuclear boundary. The direction of zonular angles can significantly influence curvature change regardless of the modulus distribution.** ***Conclusions:*** **The present paper proposes a modelling approach for the human lens, coupling optical and mechanical properties, which shows the effect of parameter choice on model response.** ***Significance:*** **This advanced modelling approach, considering the important interplay between optical and mechanical properties, has potential for use in design of accommodating implant lenses and for investigating non-biological causes of pathological processes in the lens (e.g., cataract).**

***Index Terms*—Opto-mechanical modelling, finite element analysis, human eye lens, accommodation, radial cortical Young's moduli, zonules.**

Manuscript received March 21, 2019; revised May 30, 2019; accepted July 2, 2019. Date of publication August 5, 2019; date of current version March 19, 2020. This work was supported in part by Zeiss Meditec AG, Royal Society under Grant IE160996 and beamtime grants at SPring-8 synchrotron under Grants 2014A1710, 2015A1864, and 2016A1096. *(Corresponding author: Barbara Pierscionek.)*

K. Wang is with the School of Science and Technology, Nottingham Trent University.

D. T. Venetsanos is with the School of Mechanical, Aerospace and Automotive Engineering, Coventry University.

M. Hoshino, K. Uesugi, and N. Yagi are with the Japan Synchrotron Radiation Research Institute (Spring-8).

B. K. Pierscionek is with School of Science and Technology, Nottingham Trent University, Nottingham NG11 8NS, U.K. (e-mail: barbara.pierscionek@ntu.ac.uk).

Digital Object Identifier 10.1109/TBME.2019.2927390

I. Introduction

THE eye is a complex optical and neurological system for refracting light to produce high quality images that undergo processing at the retina and further processing, via the higher visual pathways, in the visual cortex of the brain. The two refractive elements in the eye are the cornea and the lens. The cornea provides approximately two-thirds of the ocular focusing power. The lens contributes the remainder and is responsible for adjusting the refractive power of the eye, via a process called accommodation, to meet the visual demands over a range of object distances. Accommodation decreases gradually with age such that, by the sixth decade of life, the eye can no longer focus on near objects [1], [2]. This age-related process is known as presbyopia.

The lens, which is composed of a lamellar arrangement of fibre cells and contained within the semi-elastic capsule, adjusts the focus of the eye by altering its shape [3]. This is mediated by a ring of suspensory ligaments, collectively called the zonule, which is connected to the capsule around the equator of the lens and transmits the forces that alter lens shape from the ciliary body [3]. The anterior, equatorial and posterior sections of the zonule originate from different locations on the ciliary body [4]. Yet a number of modelling approaches simplify these forces as emanating from a single point [5]–[9]. Recently it was shown that separating directions of zonular force across the three sections makes a substantial difference to the shape change and renders the modelled simulation closer to the changes in shape seen in the biological lens [10]. This is fundamental for understanding the mechanical behaviour of the different zonular sections and for providing insights needed to understand the accommodative process and its loss with age. Such insights may resolve the conflicts between major accommodative theories [11]–[14]. Recent modelling [10] and experimental studies on monkey lenses [15] suggest that the equatorial zonular section is less effective when compared to the anterior and posterior zonular sections in altering central curvatures and optical power of the lens during accommodation. This has been previously postulated [12], [16].

Two regions within the lens are broadly recognised: a central nucleus that comprises approximately two-thirds of the total lens from the perspective of radial distance, and the outer cortical region [17], [18]. Whilst there is no biochemically distinct

cortico-nuclear boundary, the refractive index profile of the human lens indicates a marked difference in magnitude and variation in refractive index: there is an almost constant refractive index over the central two-thirds of the lens and a sharp gradient in the outer third (reviewed in [19]). The refractive index is linearly related to the concentrations of lens proteins according to the Gladstone-Dale formula [20] indicating that this gradient is also linearly related to that of the protein concentration profile.

Mechanical properties in the living human eye lens have been measured recently using Brillouin scattering analysis [21]. The direct relationship between refractive index and elastic modulus are not known as it has not been possible to measure both properties in the same lens. However, profiles of longitudinal elastic modulus, measured along the optic axis of the lens using *in vivo* Brillouin scattering analysis [22], bear a close resemblance to refractive index distributions from *in vitro* samples measured using a phase contrast imaging modality: X-ray Talbot interferometry [23]. Although light rays are utilized by both measuring techniques, the methods of application are different from one another. Brillouin scattering analysis relies on the frequency shift between incident light and scattered light caused by periodic modulations of refractive index by acoustic phonons [22], [24], [25]. This Brillouin shift is dependent on the propagation speed of the acoustic wave and can be converted to longitudinal modulus using the ρ/n^2 ratio (where ρ is the density and n is the refractive index) of the sample. This was found to be a constant value across the whole lens [22], [25]. The X-ray Talbot grating interferometer consists of two transmission gratings (a phase and an absorption grating) that are used to create Moiré fringe patterns of X-ray beams after traversing the sample [26]. Moiré fringes are used to determine the spatially varying protein densities across the specimen from which refractive indices are calculated using the Gladstone-Dale formula [20], [27]. Both techniques have fine resolution: 60 μm for Brillouin analysis [22] and 5.5 μm for interferometric analysis [26]. The similarity between distributions of refractive index and longitudinal modulus provides a means of creating optically relevant and mechanically viable models. Such models, with gradient profiles, are needed to improve current understanding of cataract, and to facilitate the design of optically advanced, accommodating intraocular lenses.

Almost all previous modelling studies assumed uniform distributions of material properties in the lens nucleus and cortex, and used lens models based on limited ages [5]–[9]. This study describes advanced models that correlate distributions of material properties derived from *in vitro* optical measurements of refractive index [23] with *in vivo* mechanical analyses [22]. Finite Element lens models were created based on human lenses from five different ages, covering the age range from the second to the sixth decade of life. A parametric analysis of 990 different combinations of zonular angles and hence directions of force on the lens, was conducted for each model using an exhaustive search scheme developed in a previous study [10]. The resultant changes in lens thickness and stress field distributions were analysed to investigate the opto-mechanical relationship and how this may alter with age.

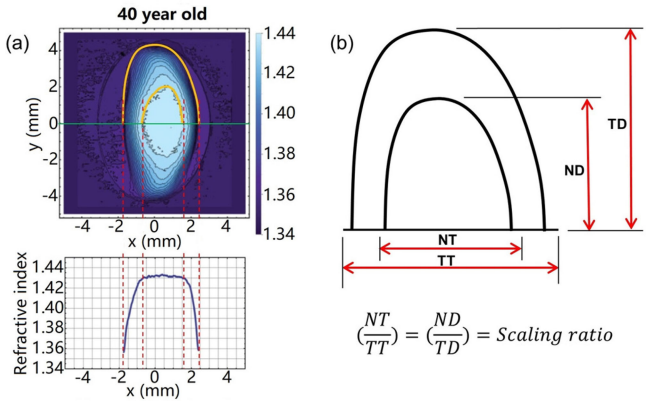

Fig. 1. Extraction of lens geometry of the 40-year-old lens [23] as an example with nuclear shape determined (a) by fitting contour corresponding to the central plateau region [23] and (b) by scaled down from the outer shape according to mechanical measurements by Besner *et al.* [22].

II. Method

Lens models were developed based on human lenses aged: 16, 35, 40, 57 and 62 years and subjected to X-ray Talbot interferometric analysis to obtain refractive index and lens shape [23]. Two distributions of cortical Young's moduli were modelled for each age: (a) a uniform distribution and (b) a radial linear *nodal* distribution calculated from the longitudinal modulus measured using *in vivo* Brillouin scattering analysis [22] on lenses that covered a similar age range as in the optical study [23].

A. Geometry of Models

Boundaries of the lens outer shape were taken from isoindicial contours of refractive index reported by Pierscionek *et al.* [23]. The contour corresponding to a minimum magnitude of refractive index, approximately 1.35 [23] was taken as the outer lens shape.

For each uniform model, the contour corresponding to the central plateau region, shown on the index profile of each lens in the sagittal plane along the central optical axes [23], was treated as the cortico-nuclear boundary. Fig. 1(a) shows an example of how these geometric parameters were extracted for a 40-year-old lens from X-ray interferometric analysis of the refractive index gradient.

For models with radially varying Young's moduli in the cortex, the nuclear boundary for each model was created by scaling the boundary of the outer lens using an age-related scaling ratio that was determined from Besner *et al.* [22]. A representative example for determining the nuclear shape by scaling is shown in Fig. 1(b) for the 40-year-old lens [23].

B. Analysis of Mechanical and Optical Data

The findings reported by Besner *et al.* [22] include detailed parameters describing the profile shapes of longitudinal moduli measured along the optical axis of each lens. For all 56 measured lenses, the Total Thickness *(TT)* and Nuclear Thickness *(NT)* can

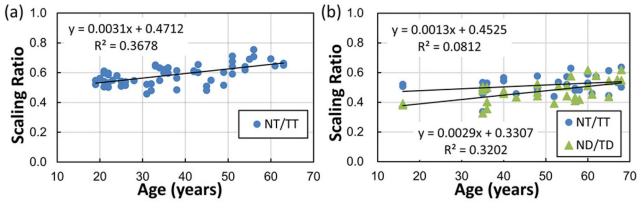

Fig. 2. Ageing trend of ratios describing nuclear to total lens proportions (a) in sagittal plane re-analyzed from Besner *et al.* [22] and (b) in both sagittal and equatorial planes re-analyzed from Pierscionek *et al.* [23].

TABLE I
SCALING RATIOS, CAPSULAR THICKNESS AND CAPSULAR ELASTICITY OF LENS MODELS AT EACH AGE

		Age				
		16	35	40	57	62
Besner [22]	*NT/TT*	0.52	0.58	0.59	0.65	0.66
Pierscionek [23]	*NT/TT*	0.52	0.45	0.54	0.49	0.57
	ND/TD	0.39	0.50	0.48	0.41	0.58
Capsular thickness [μm]		13	15	16	19	20

be determined using the following parameters:

$$NT = xc_{pos} - xc_{ant} \tag{1}$$

$$TT = L_{ant} + L_{pos} + NT \tag{2}$$

where xc_{pos}, xc_{ant}, L_{ant} and L_{pos} are parameters fully defined in [22]. The ratio *(NT/TT)* describes the nuclear to total lens thickness along the optic axis and is shown plotted against age in Fig. 2a. A linear regression analysis of data yields a relationship of $\boldsymbol{y} = 0.0031\boldsymbol{x} + 0.4712$ between age and the *(NT/TT)* ratio, where $\boldsymbol{x}$ stands for age and $\boldsymbol{y}$ stands for the *(NT/TT)* ratio. The scaling ratio used to determine shapes of lens nuclei for radial models at each age was calculated from this equation and is given in Table I.

The geometries of lenses used to measure refractive index by Pierscionek *et al*. [23], include profiles both along the optic axis and along the equatorial plane. The nuclear half-diameter (*ND*) and the total half-diameter (*TD*) for each lens were determined by measuring the central contour which corresponds to the plateau region of each refractive index profile (seen in Fig. 1(a)). The ratios (*NT/TT*) and (*ND/DD*) obtained from lens geometries for lenses up to 70 years of age are plotted against age in Fig. 2b.

C. Material Properties and Opto-Mechanical Coupling

According to the profiles of longitudinal modulus [22], the magnitude of the central plateau region for 56 lenses is within the range of 3.278 ± 0.081 GPa with no age dependency. This value decreases continuously from the central plateau region toward the anterior and posterior pole of each lens to a minimum value within the range of 2.498 ± 0.139 GPa [22]. Given that no age-related trend was observed, the average values at the central plateau and at the lens poles, 3.286 GPa and 2.471 GPa

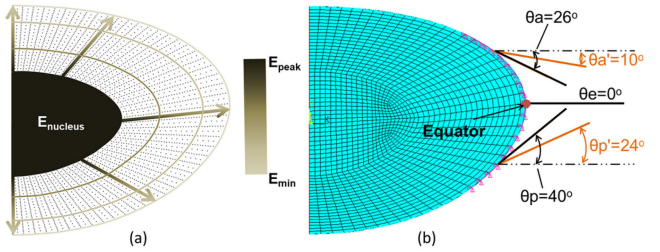

Fig. 3. (a) Illustration of the linearly varying cortical Young's modulus within the lens (the colour bar on the right side shows the decreasing values from the nuclear to the external lens boundary), (b) corresponding discretized 35-year-old model with a zonular angle triplet of [10°, 0°, 24°] (in black colour) and of [26°, 0°, 40°] (in orange colour).

respectively, were used to construct the models. Recent studies [25], [28] have derived an empirical relationship between longitudinal modulus $\boldsymbol{M}$ and conventional low frequency modulus, i.e., Young's modulus $\boldsymbol{E}$ or shear modulus $\boldsymbol{G}$. This log-log linear equation [25] is described as:

$$\log(M) = a\log(G) + b \tag{3}$$

where a and b are material dependent coefficients that were determined for porcine lenses: a = 0.093 and b = 9.29 [25] which have similar elastic shear moduli to young human lenses [29], [reviewed in 30]. Taking the eye lens as nearly incompressible [31], [32] Young's and shear modulus can be linearly related: $\boldsymbol{E} = \boldsymbol{3G}$ [10], [30]. The calculated Young's moduli $\boldsymbol{E}$ at the central plateau and at the lens poles are 0.82 kPa and 0.04 kPa respectively.

Consistent with the findings by Besner *et al.* [22], no age-related variations in material properties were considered in the present study. For both sets of models: those with uniform and those with a radial distribution of cortical Young's moduli, a value of 0.82 kPa was used in the lens nucleus. Models with a uniform cortical Young's modulus were given an average value, 0.43 kPa, of the maximum and minimum for each age. For models with radially varying cortical moduli, Young's modulus decreased linearly from 0.82 kPa in the nuclear region to 0.04 kPa at the lens surface (Fig. 3a).

All models were discretized using a mapped mesh (Fig. 3b) with 97 nodes uniformly distributed both along the cortico-nuclear boundary and the external lens surface, forming a well-aligned radially distributed pattern of 97 groups of colinear nodes (Fig. 3a). A linear interpolation of Young's modulus was used for each nodal group with the maximum value assigned to the node on the nuclear-cortical boundary and the minimum value assigned to the node on the external lens boundary. Such a distribution forms iso-indicial contours of Young's modulus, which are similar to the distributions of optical refractive index [23]. The decreasing trend of Young's modulus is indicated using arrows with changing shades for five nodal groups (Fig. 3a).

Young's modulus was taken as 1.5 MPa [33] and 0.35 MPa [34] for lens capsules and zonular fibres, respectively, for all models and Poisson's ratio of 0.47 was used for both lens

capsules [10] and zonular fibres [35]. All model sections were considered to be linear, elastic and isotropic.

D. Model Discretization and Boundary Conditions

Axisymmetric models were created in ANSYS mechanical APDL (ver.18.1). Each lens model contains six different parts: the nucleus, cortex, capsule, an anterior zonular fibre, an equatorial zonular fibre and a posterior zonular fibre. The lens nucleus and cortex were meshed using 8-node axisymmetric elements (ANSYS element type: PLANE 183, KEYOPT(3) = 1), the lens capsule was modelled using 3-node membrane elements (ANSYS element type: SHELL 209, KEYOPT(1) = 1), the three bundles of zonular fibres were considered as three 2-node elements carrying tensional loads only (ANSYS element type: SHELL 208, KEYOPT(1) = 1, KEYOPT(2) = 0). The total number of elements was 1515 and the total number of nodes was 7436 for each model. Zonular fibres were given a length of 1.5 mm and a thickness of 0.05 mm [36]. The three zonular sections were modelled such that their free endpoints were decoupled permitting movement in different directions. The coupling mechanism of the zonular-capsular anchoring points with surrounding nodes, shown in Fig. 3b, was the same as that described previously [10].

The nodes on the central axis were constrained in the horizontal direction and allowed a vertical translational degree of freedom. A total displacement of 0.5 mm [37], introduced in six even increments, was imposed on all models at the free endpoints of all zonular fibres and in the direction indicated by the orientation of a given fibre. The free endpoint of each zonular fibre had in-plane translational degrees of freedom.

E. Applied Procedure of Exhaustive Search

The present study conducted an exhaustive search scheme introduced in a previous study [10] using two joint codes developed in MatLab (ver. 2017b) and in ANSYS Mechanical APDL (ver.18.1). With the MatLab code, three angles for the anterior, equatorial and posterior bundles of zonular fibres were generated and ANSYS was used, as an external FE solver, to run in batch mode. The ANSYS code was then applied to read the three zonular angles and build corresponding lens models using predefined information, i.e., the lens geometry, material properties, element types, meshing strategy and boundary conditions. This information was stored in an input file. Once the FE simulation with ANSYS was finished, the MatLab code was used to retrieve results from the FE analysis and perform post-processing analysis. The changes in the central radius of curvature of the lens along the external boundary of the lens (taken within a central 3mm diameter zone), the Central Optical Power (COP), the sagittal thickness of the nucleus and of the whole lens were calculated during the post-processing analysis and stored in an output file. The COP was calculated using the thick lens formula assuming an equivalent refractive index of 1.42 for each lens [19], [38]. This task indicated the successful completion of one cycle of the exhaustive search. The MatLab code then generated another set of zonular angles and entered the next cycle of the exhaustive search. The domain of the anterior zonular angle θ_a (as seen in Fig. 3b) was between 10° to 28° towards the posterior of the eye (represented as [10°, 28°]); that of the equatorial zonular angle θ_e (Fig. 3b) was [−10°, 10°] (the negative sign denoting the posterior direction and the positive sign denoting the anterior direction for θ_e only) and that of posterior zonular angle θ_p (Fig. 3b) was [24°, 40°] towards the anterior of the eye. The selection of the three angular domains was such that the zonules would not merge with the lens body during simulations for all the examined models. Considering the computation resources and time required to conduct the exhaustive search within the defined domains, a step size of 2 degrees was used for each zonular angle. This resulted in 990 combinations of zonular angles included in the search procedure for each examined model.

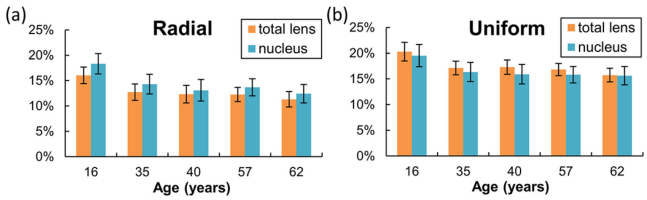

Fig. 4. Changes in lens thickness along the optic axis as percentages of the total and of the nuclear thickness plotted against age for all five aged models with (a) radial distribution of cortical Young's moduli and (b) uniform distribution of cortical Young's modulus.

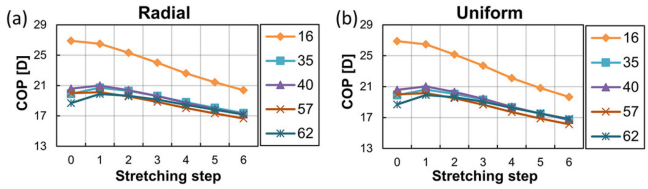

Fig. 5. Changes in Central Optical Power (COP) versus stretching for both models with a zonular angle triplet of [10°, 0°, 24°] and with both (a) radial distribution of cortical Young's modulus and (b) uniform distribution of cortical Young's modulus at all five ages.

III. Results

For each model, the changes in thickness along the optical axis as a percentage of the total lens thickness and as a percentage of the nuclear thickness were calculated for all simulated combinations of zonular angles. The values were further averaged across the 990 angular combinations and plotted against age in Fig. 4. For models with radially varying cortical Young's moduli, the nuclei are stretched to a greater degree than the total lens for all ages (Fig. 4a). Models with a uniform cortical Young's modulus show a higher percentage of change in thicknesses of both the nucleus and the total lens (Fig. 4b). The youngest lens model has a greater change in thickness (Figs. 4a, b), but the difference is only slight for the set of models with a uniform cortical Young's modulus (Fig. 4b).

Fig. 5 shows the change in COP versus the stretching increment, for each set of models. The curves correspond to models with a zonular angle triplet of [10°, 0°, 24°], i.e., the anterior, equatorial and posterior zonular angles, respectively.

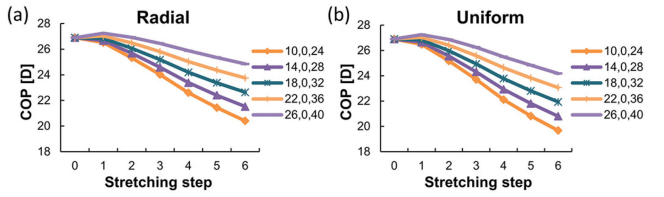

Fig. 6. Change in COP with stretching for models aged 16 years with (a) with radial distribution of cortical Young's moduli and (b) with a uniform distribution of cortical Young's modulus for 9 selected combinations of zonular angles ranging from (c) [10°, 0°, 24°] to (d) [26°, 0°, 40°].

The selection of this combination of zonular angles provided the maximum change in COP amongst all 990 tested combinations for all ages.

The 16-year-old model stands out from the others with a substantially greater change in COP for every increment of stretch and shows more variation with stretch than any of the other models (Fig. 5). This applies whether the cortex is modelled with radially varying Young's moduli (Fig. 5a) or with a uniform Young's modulus (Fig. 5b). For older aged models: 35, 40, 57 and 62 years old, there is a general decrease in COP with stretching. Notably, for both sets of models, the first stretching increment results in an increase in COP for those aged 35, 40 and 62 years, with the latter showing the most marked increase of 1.2 dioptres (Fig. 5a, b).

Fig. 6 shows the COPs of five selected zonular angle triplets plotted against stretching for the 16-year-old model. With stretching, the COP undergoes less change with more convergent zonular angles than for less convergent zonular angles and this occurs for models with both distributions of cortical Young's moduli (Fig. 6a, b). Indeed, there is negligible difference in COP change between models with a uniform or a radially varying cortical Young's moduli. The influence of the equatorial zonular angle was not included; this part of the zonule has little effect on the curvature change. This is demonstrated in Tables II and III in the Appendix.

Comparisons of changes in radii of curvature, COP and internal stress distributions between models with all three sets of zonular bundles (triplet) [10°, 0°, 24°] and with only anterior and posterior zonular bundles (doublet) [10°, 24°] are shown in Fig. 7 for the 16-year-old model with radial distribution of cortical Young's moduli. The models show the same changes in central anterior and posterior radii of curvature (Fig. 7a, b) as well as in COP (Fig. 7c) whether a triplet or doublet zonule is used. However, the model with the triplet zonule (Fig. 7d) has a greater displacement along the lens equator of 0.503 mm (the model with doublet zonule has a displacement of 0.305 mm) and higher stresses than the model with the doublet zonule (Fig. 7e) for the same degree of simulated stretch.

The internal stress (as von Mises stress in MPa) distributions for models with both radial and uniform distributions of cortical Young's moduli are shown in Fig. 8. For both sets of models, the highest stresses are seen in the lens nucleus. The stress distributions vary relatively gradually for models with radial cortical Young's moduli (Fig. 8a–e). Sharply changing stress

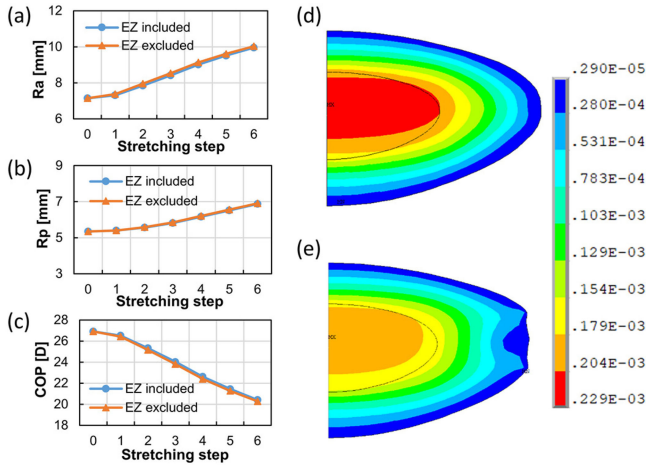

Fig. 7. Comparisons between 16-year-old radial models with the equatorial zonule (EZ) included and excluded for (a) anterior radius of curvature, (b) posterior radius of curvature, (c) Central Optical Power, and von Mises stress (MPa) of model with (d) EZ included, (e) EZ excluded.

patterns at the cortico-nuclear boundary are evident in models with uniform cortical Young's moduli (Fig. 8f–j); the greatest range of stress values is seen in the 16-year-old lens (Fig. 8f). The latter set of models have higher stress magnitudes in the lens cortex (Fig. 8f–j) than do models with radially varying cortical Young's moduli (Fig. 8a–e) for every age.

IV. Discussion

The present study proposes a modelling concept including lens models with radial distribution of cortical Young's moduli that is akin to the distribution of optical properties across the lens [23]. The same magnitude of material properties was used for lens models with different geometries based on curvatures extracted from human lenses of varying ages [23]. Brillouin scattering, which measures longitudinal modulus across lenses *in vivo*, showed that the width of the central plateau increases with age (Fig. 2a) with no change in the magnitude [22], [39]. Optical measurements of refractive index distributions demonstrated a similar trend (Fig. 2b). By comparing Young's modulus and shear modulus measured using conventional low frequency stress-strain test to longitudinal modulus measured using high-frequency Brillouin scattering analysis, Scarcelli *et al.* [25] quantified a log-log linear relationship between the two types of moduli for fresh bovine and porcine lens specimens and determined their respective fitting coefficients (a and b in equation 3). The values are different between the two species [25]. Given the scarcity of human samples from young healthy donors, such a relationship has not been determined for human lenses. However, the similar magnitudes of shear moduli between porcine and young human lenses [29], [30] render the selection of parameters in the present study the best available choice.

Applying simulated stretching of 0.5 mm at six equal increments to each zonular section, to induce changes in shape within the range measured clinically [37], [40], shows a greater

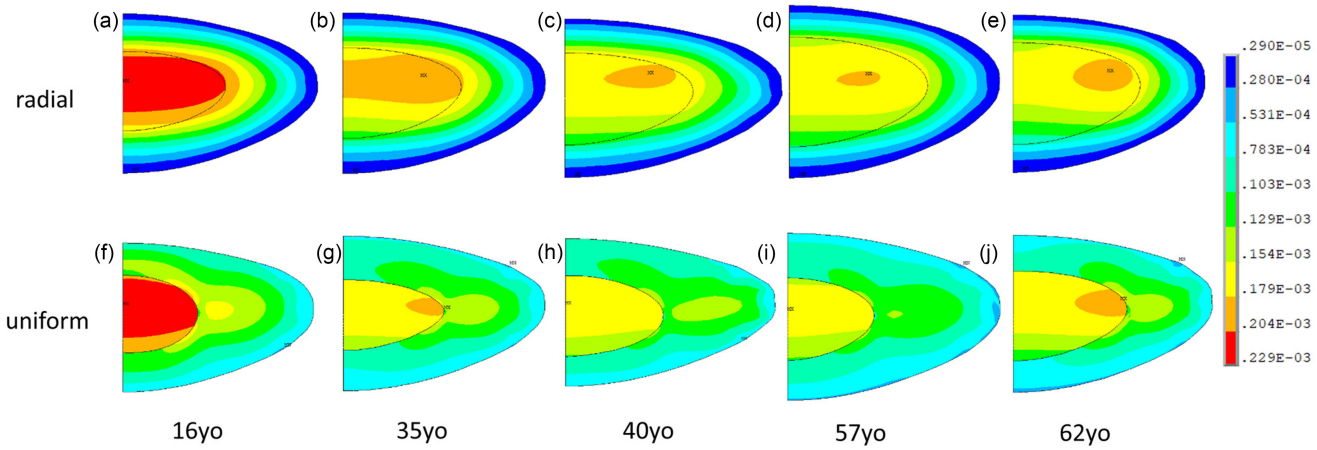

Fig. 8. Stress distributions (von Mises Stress in MPa) for models at five simulated ages with two distributions (radial and uniform) of cortical Young's modulus.

change in nuclear thickness than in total lens thickness when the cortical Young's modulus has radially varying values (Fig. 4a) This concurs with earlier observations of the lens nucleus during accommodation [17], [41], [42], [43]. The effect of a radially varying Young's modulus in the cortex is also evident with respect to deformation: a lower degree of shape change is needed to produce a similar amount of change in COP from a model with a radially varying cortical Young's modulus, compared to a uniform cortical Young's modulus (Fig. 5).

The 16-year-old model demonstrates the maximal change in COP (Fig. 5) which adheres to the physiological situation given the loss of accommodative ability with age [44]. Since all models had the same magnitude of Young's moduli, the results suggest that the shape differences are the major contributing factor for age-related differences that are found in the living eye. Current definitions of lens nucleus and cortex are inconclusive [18], [45] with the plateau region where the refractive index is constant (corresponding to a similar trend in Young's modulus) accepted as the nucleus [19], [23]. Whilst there is a hint of an increasing proportion of nucleus to total lens size with age (Fig. 2), the results show individual variations. A decrease in thickness of the total lens and of the nucleus with simulated stretching is most evident in the youngest lens and decreases, with age, for models with gradient cortical Young's moduli (Fig. 4a). This ageing change is not as apparent for models with uniform cortical moduli (Fig. 4b). Changes in thickness in response to simulated forces are indicative of changes in overall moduli of elasticity. Clearly, an increase in overall size of the lens with age does not alter the overall modulus; the presence of a gradient modulus in the cortex has a far greater effect.

The semblance of a turning point (an initial increase and then a decrease in COP with stretching) is seen in Fig. 5. The incremental increase is very small and the greatest power changes in the 62-year-old lens models are around 1.2 dioptres. It has been noted in a previous numerical modelling study on a 29-year-old lens where for a similar displacement as this study, the initial response to stretch was an increase in power of around 4 dioptres [46]. The stretching force in that study was mediated via an anterior and posterior zonule and emanated from a single point [46]. The geometries of the lens models were based on *post-mortem* lenses [23] and hence freed from tension imposed on lenses *in vivo* by the ciliary muscle and zonule. The assumption used by almost all of the previous modelling studies [5], [7], [47], [48] was that the *in vitro* lenses are in the fully accommodative state. An opposing study showing that the *post-mortem* lenses with a mean optical power of 19.8 ± 1.7 dioptres are actually in unaccommodative states [49]. The COPs of the lens models based on *in vitro* lenses (not under zonular tension) aged between 35 to 62 years were found to be around 20 dioptres when calculated using the thick lens formula [38] (Fig. 5). Further investigations are needed to better determine whether the increase in COP, at this first stretching increment, is an indication of the models entering from *post-mortem* (stress-free) states to the fully accommodative *in vivo* state (minimal stress) or rather that of lens change for low levels of accommodation, i.e., below 2 dioptres.

Results in Fig. 6 confirm that the angle at which zonular fibres mediate the force from the ciliary muscle is critical in the amount of power change and pertinent to geometrical changes with age. Recent studies [50] found that the ciliary muscle undergoes an apparent anterior and inward movement with age, which concurs with seminal work showing an anterior zonular shift with age [51]. The concomitant closer movement of different zonular attachments could contribute to the accommodative loss with age. Future designs of artificial intraocular lenses should consider the force applications and the directions of different zonular forces if there is to be any effective restoration of accommodative capacity of lenses after implant surgery.

Previous studies on two models aged 16 and 35 years, demonstrated that a closer fit to *in vivo* data [10], [52] can be obtained when modelling anterior, equatorial and posterior zonular sections with separate directions of stretch than with a single direction [10]. The equatorial zonule has significantly less influence on the change in surface curvatures and optical powers than do the anterior and posterior zonular sections [52]. This is demonstrated in the present study: models with or without the equatorial zonule have the same change in surface curvature and COP with simulated stretching (Fig. 7a–c); altering equatorial

zonular angle alone has less influence on the surface curvatures of models with both radial and a uniform cortical Young's modulus (Appendix Table II and III). However, whilst there is no change in the optics, there are differences in the mechanical factors: the stresses are greater with a zonular triplet i.e., with an equatorial component, than without (Fig. 7d, e).

Subjected to the same level of stretching, the 16-year-old model shows the greatest stresses compared to other aged models. This is because this lens has the smallest dimensions. Models with a gradient of Young's modulus in the cortex (Fig. 8a–e) show that the youngest lens has a more even distribution of stresses across the tissue and that in older models there are lower stresses but these appear as regions of relatively higher values in the equatorial region of the lens nucleus. The trend is very general given individual variations in lens size. Models with a uniform distribution of cortical Young's modulus show less consistency between stress distributions and age (Fig. 8f–j). The construction of many more models based on very large numbers of lenses, are needed to indicate any general trends.

The significant difference between models with a uniform distribution of Young's modulus in the cortex and models with radial distribution of Young's modulus in the cortex is seen with respect to the stress distributions. A model with uniform cortical Young's modulus gives a less even distribution of stress and hence higher stresses in the lens cortex than does a model with a radially varying distribution. Similar findings were reported in previous studies [52], [53]. Nonetheless, small regions of higher stress can be found in both sets of models around the cortico-nuclear boundary in the equatorial region. This area has been shown to have cortical opacities that cause light-scattering [54]. Cells are mechanosensitive [55] and they will collectively respond to regional perturbations to their environment, whether these are caused by physiological, biochemical or physical (mechanical) effects. Unlike nuclear cataract, which is a homogenous process associated with protein aggregation, cortical cataract has been related to stress damage occurring as a result of continued accommodative effort [54], [56]. The variations in cortical Young's modulus seen *in vivo* [22] and the effect of the equatorial zonule, albeit playing a lesser role in optical change with accommodation than other zonular sections, may be a biological means of protecting the lens from what would otherwise be more frequently occurring mechanically induced cataract.

V. Conclusion

We propose an approach that couples mechanical and optical properties in the construction of human lens models representing different ages and accommodative capacities. Models with cortical Young's moduli have a more uniform stress distribution and require less thickness change to produce similar refractive change than models with uniform cortical Young's moduli. Age-related changes in lens geometry are a major contributing factor to accommodative loss but do not completely explain the development of presbyopia. Simulations for a range of zonular angle combinations, indicate that attachment locations of different zonular sections to the ciliary muscle are crucial for predicting lens accommodative capacity.

TABLE II
Anterior Radius of Curvature of Undeformed and Deformed Lens Models With Two Distributions of Cortical Young's Moduli at Five Ages

Zonular angles	16	35	40	57	62
Undeformed [mm]					
	7.1	10.6	13.1	11.0	16.6
Radial model [mm]					
[10°, -6°, 24°]	9.9	12.1	12.9	12.7	13.8
[10°, 0°, 24°]	10.0	12.1	12.9	12.7	13.8
[10°, 6°, 24°]	10.0	12.1	13.0	12.7	13.8
[18°, -6°, 32°]	8.7	10.5	11.1	11.2	11.9
[18°, 0°, 32°]	8.8	10.6	11.1	11.3	11.9
[18°, 6°, 32°]	8.8	10.6	11.2	11.3	11.9
[26°, -6°, 40°]	7.7	9.2	9.6	10.0	10.3
[26°, 0°, 40°]	7.7	9.3	9.7	10.0	10.3
[26°, 6°, 40°]	7.7	9.3	9.7	10.0	10.4
Uniform model [mm]					
[10°, -6°, 24°]	10.6	13.0	13.8	13.7	14.8
[10°, 0°, 24°]	10.7	13.0	13.9	13.7	14.8
[10°, 6°, 24°]	10.7	13.0	13.9	13.7	14.9
[18°, -6°, 32°]	9.3	11.3	11.9	12.1	12.7
[18°, 0°, 32°]	9.4	11.3	12.0	12.1	12.8
[18°, 6°, 32°]	9.4	11.4	12.0	12.1	12.8
[26°, -6°, 40°]	8.2	9.9	10.3	10.6	11.0
[26°, 0°, 40°]	8.2	9.9	10.4	10.7	11.0
[26°, 6°, 40°]	8.2	9.9	10.4	10.7	11.0

TABLE III
Posterior Radius of Curvature of Undeformed and Deformed Lens Models With Two Distributions of Cortical Young's Moduli at Five Ages

Zonular angles	16	35	40	57	62
Undeformed [mm]					
	5.3	6.7	5.8	6.6	6.0
Radial model [mm]					
[10°, -6°, 24°]	6.9	7.9	7.7	8.2	7.4
[10°, 0°, 24°]	6.9	7.9	7.7	8.2	7.4
[10°, 6°, 24°]	6.9	7.9	7.7	8.2	7.4
[18°, -6°, 32°]	6.3	7.2	7.0	7.6	6.9
[18°, 0°, 32°]	6.3	7.2	7.0	7.6	6.9
[18°, 6°, 32°]	6.3	7.2	6.9	7.6	6.9
[26°, -6°, 40°]	5.8	6.7	6.4	7.1	6.4
[26°, 0°, 40°]	5.8	6.7	6.4	7.1	6.4
[26°, 6°, 40°]	5.8	6.7	6.4	7.1	6.4
Uniform model [mm]					
[10°, -6°, 24°]	7.0	8.0	7.8	8.3	7.4
[10°, 0°, 24°]	7.0	8.0	7.7	8.3	7.4
[10°, 6°, 24°]	7.0	8.0	7.7	8.2	7.4
[18°, -6°, 32°]	6.4	7.3	7.0	7.6	6.8
[18°, 0°, 32°]	6.3	7.3	7.0	7.6	6.8
[18°, 6°, 32°]	6.3	7.3	7.0	7.6	6.8
[26°, -6°, 40°]	5.9	6.8	6.4	7.1	6.4
[26°, 0°, 40°]	5.9	6.7	6.4	7.1	6.4
[26°, 6°, 40°]	5.9	6.7	6.4	7.1	6.4

Appendix

Table II presents anterior radius of curvature of lens models at all ages for nine selected combinations of zonular angles with each of two simulated distributions of cortical Young's moduli.

Table III presents posterior radius of curvature of lens models at all ages for nine selected combinations of zonular angles with each of two simulated distributions of cortical Young's moduli.

References

[1] D. Borja *et al.*, "Optical power of the isolated human crystalline lens," *Investigative Ophthalmol. Vis. Sci.*, vol. 49, no. 6, pp. 2541–2548, Mar. 2008.

[2] A. Glasser and M. C. Campbell, "Presbyopia and the optical changes in the human crystalline lens with age," *Vision Res*., vol. 38, no. 2, pp. 209–229, Jan. 1998.

[3] A. J. Bron, *Wolff's Anatomy of the Eye and Orbit*, 8th ed. Boca Raton, FL, USA: CRC Press, 1998.

[4] P. N. Farnsworth and P. Burke, "Three-dimensional architecture of the suspensory apparatus of the lens of the rhesus monkey," *Exp. Eye Res.*, vol. 25, no. 6, pp. 563–576, Dec. 1977.

[5] H. J. Burd, S. J. Judge, and J. A. Cross, "Numerical modelling of the accommodating lens," *Vis. Res.*, vol. 42, no. 18, pp. 2235–2251, Aug. 2002.

[6] H. Martin *et al.*, "Comparison of the accommodation theories of Coleman and of Helmholtz by finite element simulations," *Vis. Res.*, vol. 45, no. 22, pp. 2910–2915, Oct. 2005.

[7] A. Abolmaali, R.A. Schachar, and T. Le, "Sensitivity study of human crystalline lens accommodation," *Comput. Methods Programs Biomed.*, vol. 85, no. 1, pp. 77–90, Sep. 2007.

[8] D. van de Sompel *et al.*, "Model of accommodation: Contributions of lens geometry and mechanical properties to the development of presbyopia," *J. Cataract Refractive Surg.*, vol. 36, no. 11, pp. 1960–1971, Nov. 2010.

[9] H. M. Pour *et al.*, "Stretch-dependent changes in surface profiles of the human crystalline lens during accommodation: A finite element study," *Clin. Exp. Optometry*, vol. 98, no. 2, pp. 126–137, Mar. 2015

[10] K. Wang *et al.*, "The importance of parameter choice in modelling dynamics of the eye lens," *Sci. Rep.*, vol. 7, no. 1, Nov. 2017, Art. no. 16688.

[11] H. V. Helmholtz, "Uber die Akkommodation des Auges," *A. v. Graefe's Arch. Klin. Ophthalmol.*, vol. 1, pp. 1–74, 1855.

[12] R. A. Schachar, "Zonular function: A new hypothesis with clinical implications," *Ann. Ophthalmol.*, vol. 26, no. 2, pp. 36–38, Mar–Apr. 1994.

[13] M. Tscherning, *Physiologic Optics: Dioptrics of the Eye, Functions of the Retina, Ocular Movements and Binocular Vision*, Carl Weiland, Ed. The Keystone, 1904, pp. 183–189.

[14] D. J. Coleman, "Unified model for accommodative mechanism," *Amer. J. Ophthalmol.*, vol. 69, no. 6, pp. 1063–1079, Jun. 1970.

[15] D. Nankivil *et al.*, "The zonules selectively alter the shape of the lens during accommodation based on the location of their anchorage points," *Investigative Ophthalmol. Vis. Sci.*, vol. 56, no. 3, pp. 1751–1760, Feb. 2015.

[16] R. A. Schachar, *The Mechanism of Accommodation and Presbyopia*. Amsterdam, The Netherlands: Kugler Publications, 2012.

[17] N. Brown, "The change in shape and internal form of the lens of the eye on accommodation," *Exp. Eye Res.*, vol. 15, no. 4, pp. 441–459, Apr. 1973.

[18] J. M. Sparrow *et al.*, "The Oxford clinical cataract classification and grading system," *Int. Ophthalmol.*, vol. 9, no. 4, pp. 207–225, Dec. 1986.

[19] B. K. Pierscionek and J. W. Regini, "The gradient index lens of the eye: An opto-biological synchrony," *Prog. Retinal Eye Res.*, vol. 31, no. 4, pp. 332–349, Jul. 2012.

[20] J. H. Gladstone and T. Dale, "Researches on the refraction, dispersion, and sensitiveness of liquids," *Philos. Trans. R. Soc. Lond.,* vol. 153, pp. 317–343, Jan. 1863.

[21] G. Scarcelli and S. H. Yun, "In vivo Brillouin optical microscopy of the human eye," *Opt. Express*, vol. 29, no. 8, pp. 9197–9202, Apr. 2012.

[22] S. Besner *et al.*, "In vivo Brillouin analysis of the aging crystalline lens," *Investigative Ophthalmol. Vis. Sci.*, vol. 57, no. 13, pp. 5093–5100, Oct. 2016.

[23] B. K. Pierscionek *et al.*, "The eye lens: Age-related trends and individual variations in refractive index and shape parameters," *Oncotarget*, vol. 6, no. 31, pp. 30532–30544, Oct. 2015.

[24] G. Scarcelli and S. H. Yun, "Confocal Brillouin microscopy for three-dimensional mechanical imaging," *Nature Photon.*, vol. 2, no. 1, pp. 39–43, Jan. 2008.

[25] G. Scarcelli, P. Kim, and S. H. Yun, "In vivo measurement of age-related stiffening in the crystalline lens by Brillouin optical microscopy," *Biophys. J.*, vol. 101, no. 6, pp. 1539–1545, Sep. 2011.

[26] M. Hoshino *et al.*, "Optical properties of in situ eye lenses measured with X-ray talbot interferometry: A novel measure of growth processes," *PLoS One*., vol. 6, no. 9, Sep. 2011, Art. no. e25140.

[27] R. Barer and S. Joseph, "Refractometry of living cells. Part 1. Basic principles," *J. Cell Sci.*, vol. 3, no. 32, pp. 399–423, Dec. 1954.

[28] G. Scarcelli *et al.*, "Noncontact three-dimensional mapping of intracellular hydro-mechanical properties by Brillouin microscopy," *Nature Methods*, vol. 12, no. 12, pp. 1132–1134, Dec. 2015.

[29] R.A. Schachar, R.W. Chan, and M. Fu, "Viscoelastic shear properties of the fresh porcine lens," *Brit. J. Opthalmol.*, vol. 93, no. 3, pp. 366–368, Mar. 2007.

[30] K. Wang and B.K. Pierscionek, "Biomechanics of the human lens and accommodative system: Functional relevance to physiological states," *Prog. Retinal Eye Res.,* 2018.

[31] E. A. Hermans *et al.*, "Constant volume of the human lens and decrease in surface area of the capsular bag during accommodation: An MRI and Scheimpflug study," *Investigative Ophthalmol. Vis. Sci.*, vol. 50, no. 1, pp. 281–289, Jan. 2009.

[32] J. F. Koretz and G. H. Handelman, "A model for accommodation in the young human eye: The effects of lens elastic anisotropy on the mechanism," *Vis. Res*., vol. 23, no. 12, pp. 1679–1686, 1983.

[33] S. Krag and T. T. Andreassen, "Mechanical properties of the human posterior lens capsule," *Investigative Ophthalmol. Vis. Sci.*, vol. 44, no. 2, pp. 691–696, Feb. 2003.

[34] R. F. Fisher, "The ciliary body in accommodation," *Trans. Ophthalmol. Soc. U.K.*, vol. 105, no. Pt 2, pp. 208–219, 1986.

[35] G. van Alphen and W. P. Graebel, "Elasticity of tissues involved in accommodation," *Vis. Res.*, vol. 31, no. 7–8, pp. 1417–1438, 1991.

[36] L. A. Levin *et al.*, *Adler's Physiology of the Eye E-Book*, 11th ed. Amsterdam, The Netherlands: Elsevier, 2011.

[37] S. A. Strenk *et al.*, "Age-related changes in human ciliary muscle and lens: A magnetic resonance imaging study," *Investigative Ophthalmol. Vis. Sci.*, vol. 40, no. 6, pp. 1162–1169, May. 1999.

[38] C. E. Jones, D. A. Atchison, and J. M. Pope, "Changes in lens dimensions and refractive index with age and accommodation," *Optometry Vis. Sci.*, vol. 84, no. 10, pp. 990–995, Oct. 2007.

[39] S. T. Bailey *et al.*, "Light-scattering study of the normal human eye lens: elastic properties and age dependence," *IEEE Trans. Biomed. Eng.*, vol. 57, no. 12, pp. 2910–2917, Dec. 2010.

[40] R. F. Fisher, "The ciliary body in accommodation," *Trans. Ophthalmol. Soc. U.K.*, vol. 105, no. Pt2, pp. 208–219, 1986.

[41] B. Patnaik, "A photographic study of accommodative mechanisms: Changes in the lens nucleus during accommodation," *Investigative Ophthalmol. Vis. Sci.*, vol. 6, no. 6, pp. 601–611, Dec. 1967.

[42] J. F. Koretz, C. A. Cook, and P. L. Kaufman, "Accommodation and presbyopia in the human eye," *Investigative Ophthalmol. Vis. Sci.*, vol. 38, no. 3, pp. 569–578, Mar. 1997.

[43] M. Dubbelman *et al.*, "Changes in the internal structure of the human crystalline lens with age and accommodation," *Vis. Res*., vol. 43, no. 22, pp. 2363–2375, Oct. 2003.

[44] A. Duane, "Normal values of the accommodation at all ages," *J. Amer. Med. Assoc.*, vol. 59, no. 12, pp. 1010–1013, Sep. 1912.

[45] P. J. Donaldson *et al.*, "The physiological optics of the lens," *Prog. Retinal Eye Res.*, vol. 56, pp. e1–e24, Jan. 2017.

[46] R. A. Schachar and A. J. Bax, "Mechanism of human accommodation as analyzed by nonlinear finite element analysis," *Ann. Ophthalmol.*, vol. 33, no. 2, pp. 103–112, Jun. 2001.

[47] H. A. Weeber and R. G. van der Heijde, "Internal deformation of the human crystalline lens during accommodation," *Acta Ophthalmol*., vol. 86, no. 6, pp. 642–647, Sep. 2008.

[48] E. A. Hermans *et al.*, "Estimating the external force acting on the human eye lens during accommodation by finite element modelling," *Vis. Res*., vol. 46, no. 21, pp. 3642–3650, Oct. 2006.

[49] R. A. Schachar, "Central surface curvatures of postmortem-extracted intact human crystalline lenses: Implications for understanding the mechanism of accommodation," *Ophthalmology*, vol. 111, no. 9, pp. 1699–1704, Sep. 2004.

[50] A. L. Sheppard and L. N. Davies, "The effect of ageing on in vivo human ciliary muscle morphology and contractility," *Investigative Ophthalmol. Vis. Sci.*, vol. 52, no. 3, pp. 1809–1816, Mar. 2011.

[51] P. N. Farnsworth and S. E. Shyne, "Anterior zonular shifts with age," *Exp. Eye Res.*, vol. 28, no. 3, pp. 291–297, Apr. 1979.

[52] K. Wang *et al.*, "Gradient moduli lens models: How material properties and application of forces can affect deformation and distributions of stress," *Sci. Rep.*, vol. 6, Aug. 2016, Art. no. 31171.

[53] A. Belaidi and B. K. Pierscionek, "Modeling internal stress distributions in the human lens: Can opponent theories coexist?," *J. Vis.*, vol. 7, no. 1, pp. 1–12, Aug. 2007.

[54] R. Michael *et al.*, "Morphology of age-related cuneiform cortical cataracts: The case for mechanical stress," *Vis. Res*., vol. 48, no. 4, pp. 626–634, Feb. 2008.

[55] C. Kung, "A possible unifying principle for mechanosensation," *Nature*, vol. 436, no. 7051, pp. 647–654, Aug. 2005.

[56] R. Michael and A. J. Bron, "The ageing lens and cataract: A model of normal and pathological ageing," *Philos. Trans. R. Soc. Lond. B. Biol. Sci.*, vol. 366, no. 1568, pp. 1278–1292, Apr. 2011.